JOC The Journal of Organic Chemistry

pubs.acs.org/joc Article

Nucleophilicity Prediction *via* Multivariate Linear Regression Analysis

Manuel Orlandi,* Margarita Escudero-Casao, and Giulia Licini

Cite This: *J. Org. Chem.* 2021, 86, 3555−3564 Read Online

ACCESS | Metrics & More | Article Recommendations | Supporting Information

ABSTRACT: The concept of nucleophilicity is at the basis of most transformations in chemistry. Understanding and predicting the relative reactivity of different nucleophiles is therefore of paramount importance. Mayr's nucleophilicity scale likely represents the most complete collection of reactivity data, which currently includes over 1200 nucleophiles. Several attempts have been made to theoretically predict Mayr's nucleophilicity parameters *N* based on calculation of molecular properties, but a general model accounting for different classes of nucleophiles could not be obtained so far. We herein show that multivariate linear regression analysis is a suitable tool for obtaining a simple model predicting *N* for virtually any class of nucleophiles in different solvents for a set of 341 data points. The key descriptors of the model were found to account for the proton affinity, solvation energies, and sterics.

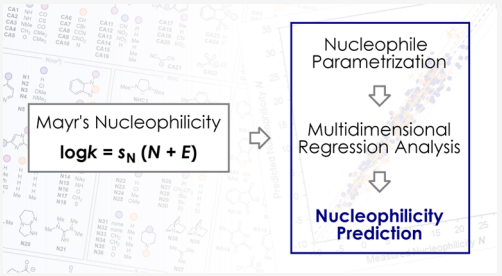

INTRODUCTION

The term nucleophile (and electrophile) was first introduced by Ingold in 1933.[1,2] Since then, the field of physical organic chemistry has grown shaping the thinking of organic chemists, and the concept of nucleophilicity established roots becoming one of the basis of organic chemistry. In the attempt to establish general reactivity rules, several groups developed different nucleophilicity scales. The Swain−Scott[3] and the Ritchie[4,5] equations are examples of early contributions in the field. However, a more general scale was more recently found to rely on the Mayr−Patz[6,7] equation (eq 1)

$$\log k\ (20\ ^\circ\mathrm{C}) = s_N(N + E) \quad (1)$$

where k is the reaction rate constant, N is the nucleophilicity parameter, E is the electrophilicity parameter, and s_N is a nucleophile-specific sensitivity parameter. Equation 1 was found to provide linear correlations for more than 1200 nucleophiles and 330 electrophiles over a reactivity range greater than 35 orders of magnitude.[7c] The reasons for such long linear correlations and the physical basis of these parameters are still not fully understood.[7d,8] However, the advantages provided by the Mayr−Patz reactivity scale from an experimental perspective are unquestionable.[9] Given N, s_N, and E for two reaction partners, it is possible to predict semi-quantitatively their reaction rate constant k at 20 °C. Moreover, comparison of N for different nucleophiles (or E for different electrophiles) gives direct evaluation of their relative reactivity.

The determination of N and s_N parameters from experimentally measured rate data for a nucleophile requires the kinetic analysis of the reaction with a series of suitable reference electrophiles of known electrophilicity E.[6a,7d] However, this experimental procedure is time-consuming in the context of predicting/screening the reactivity of compounds outside the database. Given the increasing precision of quantum chemical calculations, the kinetics and thermodynamics of most organic reactions can now be evaluated in reasonable time. Therefore, several groups employed computational methods to evaluate Mayr's reactivity parameters for different species. The groups of Houk and Mayr reported that the electrophilicities E of benzhydrylium ions correlate with their affinities for CH_3^-, OH^-, and H^-.[8a] Contreras, Pérez, Gázquez, and Fujiyama explored interesting trends between E and N with hard and soft acids and bases theory (HSAB) indices.[10] Fu and Liu evaluated N, s_N, and E for a set of nucleophiles and electrophiles by reproducing the experimental procedure *in silico via* calculation of reaction energy barriers.[8d] These studies showed that benzhydrylium electrophilicities E correlate with simple descriptors such as the lowest unoccupied molecular orbital (LUMO) energy or the Mulliken atomic charge at the electrophilic C atom. However, Michael acceptors did not follow the same trend and were shown to correlate with their methyl anion affinities instead.[8a,11] Similarly, nucleophiles provided fair correlations with the highest occupied molecular orbital (HOMO) energy

Received: December 15, 2020
Published: February 3, 2021

https://dx.doi.org/10.1021/acs.joc.0c02952
J. Org. Chem. 2021, 86, 3555−3564

only when divided in structurally similar subsets over a relatively small range of N values. A general correlation accounting for different types of nucleophiles could not be found so far. This is likely due to the structural diversity of nucleophiles in the database with respect to the electrophiles. In fact, these include π-, n-, and σ-nucleophiles of different functional groups, charges (neutral or anionic nucleophiles), and steric properties. Thus, in order to access a general and simple approach for the prediction of nucleophilic reactivity, we reasoned that such a variety of features affecting reactivity would be better described by a multidimensional correlation. Ideally, each electronic, steric, or solvation factor affecting nucleophilicity could be described by an appropriate parameter and embodied into a polynomial equation *via* multivariate regression analysis as described by Sigman and co-workers.[12] Analysis of the model equation obtained could also provide insights regarding the significance of each descriptor for a given class of nucleophiles, thus deciphering the origin of its reactivity (Figure 1).[12]

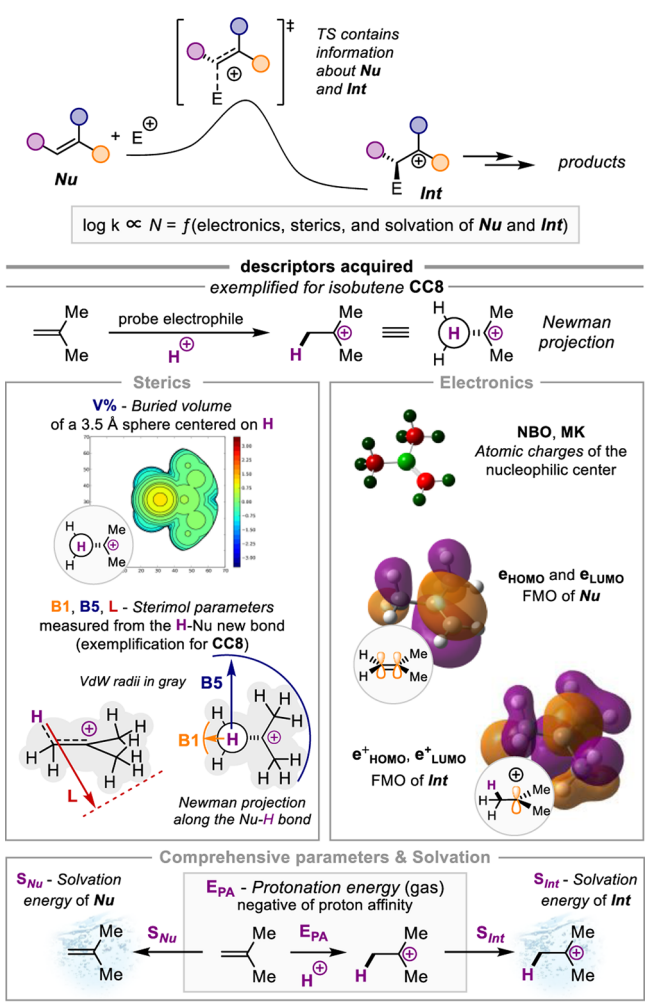

Figure 1. Rational of the work and parameters obtained.

According to eq 1, relative nucleophilic reactivities are controlled not only by the nucleophilicity parameter N but also by the susceptibility s_N, with the consequence that a nucleophile A which reacts faster than B with one electrophile may react slower than B with another electrophile. This is graphically translated in line crossings in log k versus E correlations.[7a,b] However, by using a floating scale of reference electrophiles for determining N according to eq 1, far-reaching extrapolations are avoided with the result that the nucleophilicity parameter N represents a good approximation for average nucleophilic reactivities. Being aware of this limitation, we will focus on the interpretation of N in this work and refer to the Supporting Information for evaluation of $N{\cdot}s_N$ as a possible alternative.

RESULTS AND DISCUSSION

The diversity of these nucleophiles poses a challenge for their parameterization as this is most often performed on sets of similar compounds in order to avoid biases given by major perturbations to the structure.[8d,10] How can steric descriptors be calculated consistently for different classes of compounds? For instance, which bond should be chosen for obtaining steric parameters in olefins to obtain meaningful description of sterics when compared to NHCs or amines? To solve this problem, we reasoned that consistent parameters could be calculated from the "electrophile perspective". Therefore, the structure of the protonated nucleophiles (***Int***, Figure 1) was optimized at the M06-2X/def2TZVP level of theory alongside with the plain nucleophile structures (***Nu***, Figure 1). In the general structure ***Int***, the proton **H** represents a probe electrophile which is common for every nucleophile (N is independent from the electrophile) and allows for obtaining consistent parameters through the whole nucleophile data set. The computed parameters include the following (Figure 1): % **V**, buried volume of a sphere centered on the electrophile **H** in ***Int***;[13] **B1** and **B5**, sterimol minimum and maximum width of the nucleophile, respectively, measured from the **H**−***Nu*** bond in ***Int*** considering atomic van der Waals radii (i.e., least and most distant points from the ***Nu***−**H** bond trajectory of the van der Waals isosurface's projection on the plane orthogonal to ***Nu***−**H**); **L**,[14] sterimol length of the nucleophile measured from the **H**−***Nu*** bond in ***Int***;[14] **NBO** and **MK**, natural bond orbital[15] and Merz−Kollman[16] charges of the nucleophilic atom in ***Nu***, respectively; $\mathbf{e}_{HOMO}$ and $\mathbf{e}_{LUMO}$, HOMO and LUMO energies of ***Nu***, respectively; $\mathbf{e}^{+}_{HOMO}$ and $\mathbf{e}^{+}_{LUMO}$, HOMO and LUMO energies of ***Int***, respectively;[17] $\boldsymbol{\mu}$ and $\boldsymbol{\eta}$, chemical potential and hardness of ***Nu*** according to HSAB, respectively;[18] $\mathbf{E}_{PA}$, protonation energy of ***Nu*** (calculated as the difference between the electronic energy of ***Int*** and ***Nu***), that is, the negative of the proton affinity; $\mathbf{S}_{Nu}$, $\mathbf{S}_{Int}$, and $\mathbf{S}_{H}$, solvation energy of ***Nu***, ***Int***, and H^+, respectively, calculated by single-point energy calculation at the M06-2X/def2TZVP [SMD = solvent] level on the M06-2X/def2TZVP structure optimized in the gas phase.[19] Additional convenient descriptors were added to the parameter matrix in order to provide possible corrections to the models. These are **q**, the nucleophile charge accounting for rough electrostatic effects, and $\boldsymbol{\varepsilon}$, the solvent dielectric constant.

We obtained these parameters for 264 nucleophiles in different solvents for a total number of 341 data points from Mayr's data set, which include 41 olefins,[7b,20] 38 (hetero)-aromatics,[7b,20,21] 22 Si-enolates (silyl ketene acetals, silyl enol ethers),[7b,20,22] 35 enamines,[7b,20a,23] 26 ylides,[24] 5 NHCs,[25] 31 anionic C-nucleophiles (carbanions),[26] 67 N-nucleophiles (aliphatic amines, pyridines, imidazoles, etc.),[7c,e,27] 27 anionic N-nucleophiles,[28] 41 O-nucleophiles (phenolates and carboxylates),[29a,b] and 8 S-nucleophiles.[29c,d] These were chosen over a nucleophilicity range of 35 N units in 7 different solvents (DCM, ACN, THF, acetone, DMF, DMSO, and water). The

https://dx.doi.org/10.1021/acs.joc.0c02952
J. Org. Chem. 2021, 86, 3555−3564

Chart 1. Nucleophiles Included in This Study

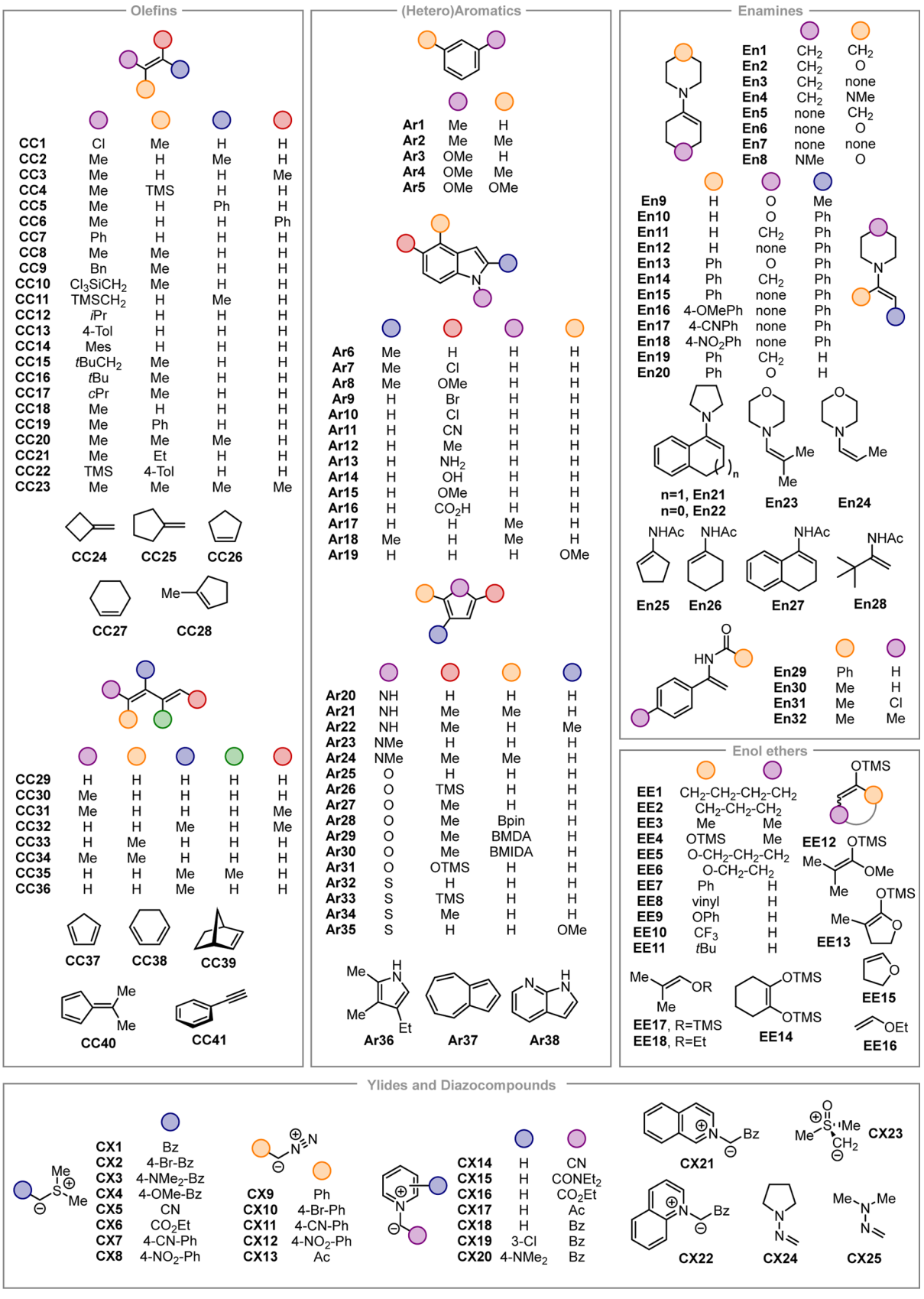

https://dx.doi.org/10.1021/acs.joc.0c02952
J. Org. Chem. 2021, 86, 3555−3564

Chart 1. continued

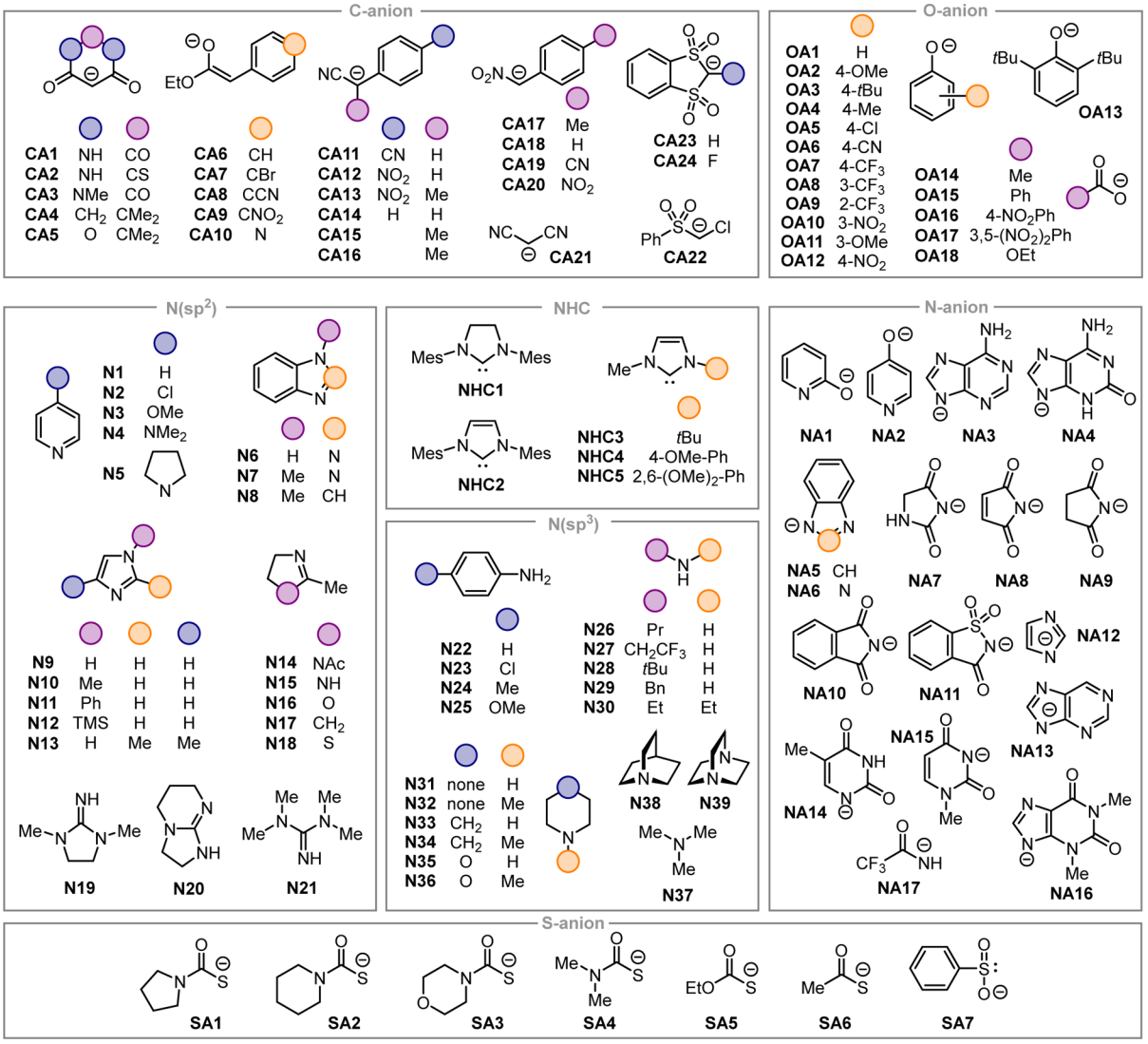

full list of the nucleophiles included in this study is given in Chart 1.

Preliminary analysis of the computed descriptors *via* single-parameter correlation against N showed that $\mathbf{E_{PA}}$ provides a good basis for further multidimensional modeling. The plot reported in Figure 2a shows a fair correlation ($R^2 = 0.86$) when removing anionic and N(sp^3)-nucleophiles from the data set. Interestingly, this latter subset gave a parallel trend with a similar slope. Anionic nucleophiles follow a separate trend and do not correlate. As recently shown by Van Vranken in the context of electrophilicity E,[11b] this is due to stronger solvation effects at place in the case of charged species. Upon addition of solvation descriptors $\mathbf{S}_{Nu}$ and $\mathbf{S}_{Int}$ to $\mathbf{E_{PA}}$, the raw model in Figure 2b is obtained (eq 2). Thus, inclusion of solvent effects increased the quality of the fit ($R^2 = 0.87$) and allowed maintaining all the nucleophiles into the same correlation. Aiming at deeper understanding of the factors implicated in the correlation between N and $\mathbf{E_{PA}}$, we performed a multivariate linear regression analysis using $\mathbf{E_{PA}}$ as the observable and the other acquired descriptors as the parameters. Since $\mathbf{E_{PA}}$ is the difference between the energies of ***Int*** and ***Nu*** by definition, it is not surprising that the regression rendered a linear combination of $\mathbf{e}_{HOMO}$ and $\mathbf{e}^{+}_{LUMO}$ with similar coefficients ($R^2 = 0.98$, Figure 3).[17]

This suggests that $\mathbf{E_{PA}}$ (and therefore N) depends not only on the activation of the reagent ***Nu*** (high $\mathbf{e}_{HOMO}$) but also on the electronic stabilization of the product ***Int*** (high $\mathbf{e}^{+}_{LUMO}$). The highlighted data points in the plot (orange crosses) identify those cases in which the LUMO of ***Int*** does not correspond to the reacting MO. These can be corrected to the shown values by changing such $\mathbf{e}^{+}_{LUMO}$ values with the energy of the MO corresponding to the formed σ^* orbital (see the Supporting Information). Interestingly, even though $\mathbf{e}_{HOMO}$ and $\mathbf{e}^{+}_{LUMO}$ are related ($\mathbf{e}^{+}_{LUMO}$ is obtained by mixing $\mathbf{e}_{HOMO}$ into the electrophile's LUMO), these two parameters do not correlate among them for the whole data set (see the Supporting Information).

Equation 2 in Figure 2b allows establishing a simple linear free-energy relationship. According to the thermodynamic cycle for a generic protonation reaction in the solvent phase (s), eq 3 holds, where thermal and entropic factors are neglected in $\mathbf{E_{PA}}$.[30]

https://dx.doi.org/10.1021/acs.joc.0c02952
J. Org. Chem. 2021, 86, 3555−3564

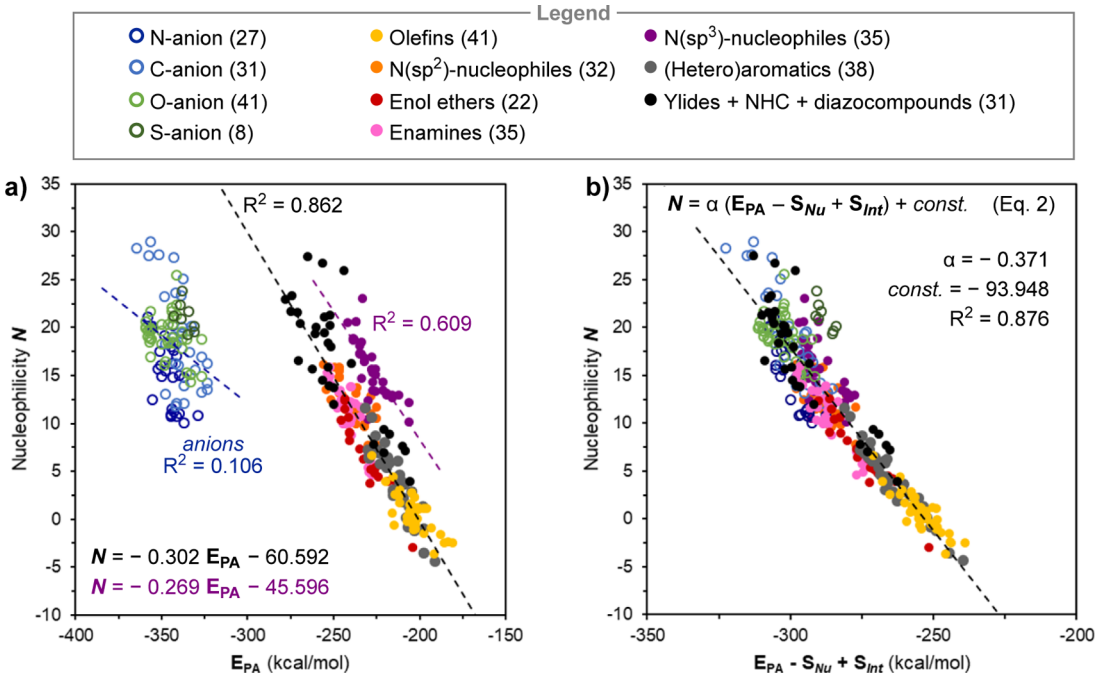

Figure 2. (a) Correlation between the nucleophilicity N and the proton affinity E_{PA} of the nucleophiles. (b) Raw model obtained by adding solvation effects to E_{PA}. The number of data points for each class of compounds is reported in parenthesis.

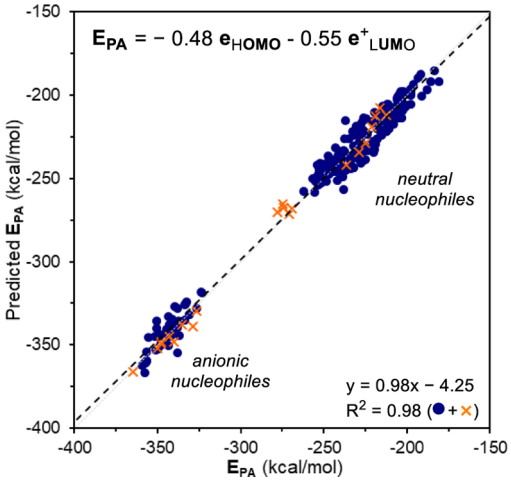

Figure 3. Correlation showing the major contribution of e_{HOMO} and e^{+}_{LUMO} to the parameter E_{PA}. Orange crosses refer to those nucleophiles for which the *Nu*−H σ^* orbital energy was considered instead of e^{+}_{LUMO} (vide infra).

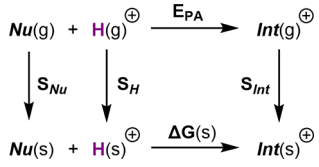

$$\Delta_R G(s) \approx E_{PA} - S_{Nu} - S_H + S_{Int} \quad (3)$$

Substitution with N according to eq 2 gives eq 4, which upon differentiation with respect to the nucleophile structural variation gives eq 5

$$\alpha\Delta_R G(s) \approx N - \alpha S_H + \text{const.} \quad (4)$$

$$\alpha\Delta_R G(s) \approx \delta N \quad (5)$$

Equation 5 is reminiscent of the linear free-energy relationship $\alpha\delta\Delta G = \delta\Delta G^{\ddagger}$, where N, being proportional to log k, is also related to $\Delta G^{\ddagger}(s)$. Thus, eq 2 correlates N with a set of parameters reproducing the nucleophile computed relative pK_a's. This could explain why S-nucleophiles are moderate outliers in the plot in Figure 2b as these are known to follow a reversed H- versus C-basicity trend with respect to O-nucleophiles, for instance.[31a] This is likely due to solvation factors as Arnett showed that in the gas phase, Me_2S and MeSH have higher proton affinity than Me_2O and MeOH, respectively.[31b] For this reason, the methyl cation affinity was computed for a subset of 96 nucleophile/solvent combinations including all the S-nucleophiles. However, these were found to follow a similar trend to the proton affinities without providing any improvement (see the Supporting Information).

The correlation in Figure 2b is in line with previous work by Bordwell and co-workers, who found a correlation between the nucleophilicity toward butyl chloride and the pK_a of a set of fluorene-derived anionic nucleophiles.[32] Interestingly, they also found that different sets of nucleophiles follow different correlations depending on steric effects.[32] Mayr and co-workers found several correlations between N and experimental pK_a values. However, they showed in different instances that such correlations are dependent on several experimental factors including the steric and solvent.[33] This prompted us to include additional parameters into our correlation *via* multidimensional correlation analysis in order to access an increased predictive power.

We divided randomly our data set into a training set (222 data points) and an external validation set (119 data points). Submitting the N array and the parameter matrix of the training set to multivariate linear regression resulted in the model depicted in Figure 4 (eq 6). In addition to E_{PA}, S_{Nu}, and S_{Int}, the parameters **q**, **B1**, **% V**, e_{HOMO}, ε, and S_H were found to be relevant descriptors for N (see the Supporting

https://dx.doi.org/10.1021/acs.joc.0c02952
J. Org. Chem. 2021, 86, 3555−3564

$$N = -2.84\,E_{PA} + 1.93\,S_{Nu} - 1.63\,S_{Int} + 0.20\,S_H - 0.07\,\varepsilon + 0.38\,e_{HOMO} + 0.98\,q + 0.18\,B1 - 0.17\,\%V \quad \text{(Eq. 6)}$$

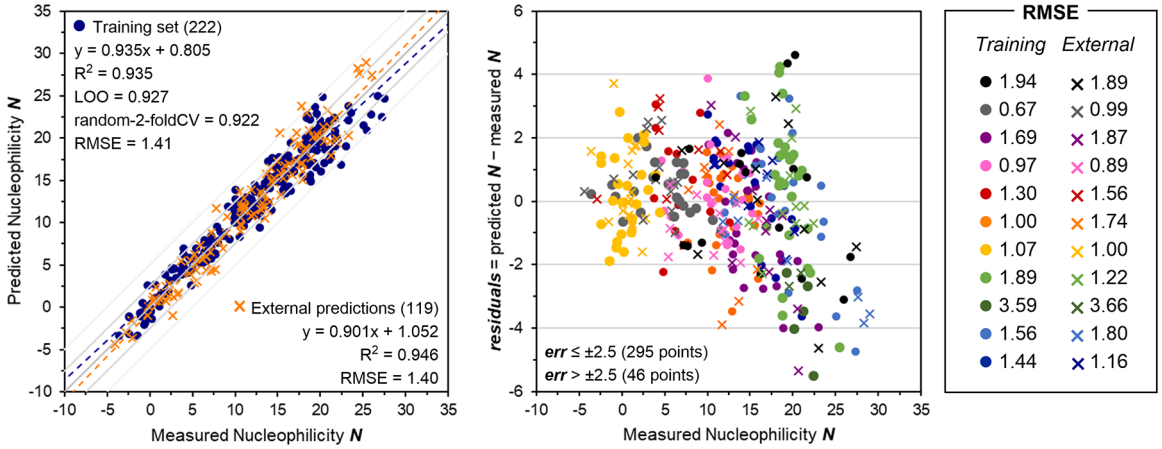

Figure 4. (a) Multidimensional model for Mayr's nucleophilicity (training set: blue dots) and cross validation by external predictions (orange crosses). (b) Analysis of the residuals plotted by the nucleophile class as the training set (dots) or external predictions (crosses). For the color legend, see Figure 2.

Information). **B1** and **% V** describe the steric hindrance of the nucleophile and suggest this to impact its reactivity. The magnitude of the coefficients (0.18 and −0.17 for **B1** and **% V**, respectively) suggests that steric effects are much less important than electronics in this instance. It is worth mentioning that the combination of steric parameters rendered by the multivariate regression procedure is not a general representation of the nucleophile steric hindrance. This is related to the steric effects arising when the nucleophile is combined with benzhydrylium cations (or structurally related quinone methides). Different steric effects may be expected to impact the reaction rate when used in combination with a different set of electrophiles![34] Such effects also include noncovalent interactions that can be specific for each nucleophile−electrophile pair.[35] Additional considerations can be made concerning the inclusion of the other parameters. The correlation in Figure 2b, on which the multidimensional model is based, is purely thermodynamic in nature. That is, the kinetic behavior of different nucleophiles is correlated with a thermodynamic property: the pK_a. This is a limitation as it is known that in some cases, Marcus' intrinsic barriers $\mathbf{\Delta G_0^{\ddagger}}$ are not colinear and not negligible with respect to the reaction free energy $\mathbf{\Delta G_0}$. This plays a crucial role in ambident reactivity.[29d,36] Mayr's N values also bring information regarding the solvation energy of the reference electrophile, the E value of which is defined to be independent from the solvent. In addition, N, s_N, and E are derived *via* fitting of experimental k-values, and the parameters calculated hereby are dependent on the used computational method. These procedures do not come without errors. These considerations provide a rationalization for the requirement for additional parameters that are needed to provide fine tuning of the model ($\mathbf{q}$, $\mathbf{e_{HOMO}}$, $\boldsymbol{\varepsilon}$, and $\mathbf{S_H}$).

Our model shows an excellent quality of fit (R^2 = 0.935, Figure 4a) and robustness as suggested by cross validation analyses (leave-one-out, Q^2 = 0.927 and average-2-fold, Q^2 = 0.922). Moreover, the root-mean-square error (RMSE) associated to the fitting is as low as 1.41, suggesting good predictive quality. The much lower RMSE given by eq 6 compared to the one provided by eq 2 (2.56) supports the requirement for the additional parameters for fine tuning of the nucleophilicity description.

Prediction of the nucleophilicities of the validation set with the model eq 6 resulted in a fit with similar properties to the training set (R^2 = 0.946 and RMSE = 1.40). The plot of the residuals for both training (circles) and validation sets (crosses) is reported in Figure 4b and divided in subsets according with the color legend in Figure 2b. The residual plot shows that the error roughly increases with the nucleophilicity, thus making prediction of anionic nucleophiles more challenging. Modeling of the product $N{\cdot}s_N$ showed that this could arise from neglecting s_N for strong nucleophiles as the sensitivity parameter becomes more important as the nucleophilicity N increases (see the Supporting Information). The RMSE for each class of nucleophiles is also reported in Figure 4. Overall, the nucleophilicity of 295 nucleophiles (87% of the set explored) could be predicted with an error <2.5 units.

CONCLUSIONS

In summary, we have shown that parameterization of a variety of nucleophiles featuring a wide structural diversity is possible. This adds to recent advances into the development of holistic multidimensional models.[37] Multivariate linear regression analysis of Mayr's nucleophilicity N with the acquired parameters allowed establishing a multidimensional model accounting for the reactivity of >300 nucleophiles over a range of 35 orders of magnitude. The model is statistically sound and provides high predicting power (RMSE < 1.5). Moreover, the descriptors appearing in the model are informative regarding the key factors affecting nucleophilicity. The nucleophile proton affinity ($-\mathbf{E_{PA}}$) and the solvation energy of both the nucleophile ($\mathbf{S_{Nu}}$) and the addition product ($\mathbf{S_{Int}}$) appear as the main parameters. As these were shown to coincide with the pK_a, this suggests that thermodynamics is a key factor contributing to the reaction rate constant k in agreement with the Bell−Evans−Polanyi principle.

However, other minor parameters were rendered by multidimensional correlation analysis, which account for several effects such as solvation, sterics, and electrostatic attraction that might play a role at the level of intrinsic activation energies (e.g., deviations from the Bell−Evans−Polanyi principle according with the Marcus theory). We also showed that $\mathbf{E_{PA}}$ can be decomposed into two major

https://dx.doi.org/10.1021/acs.joc.0c02952
J. Org. Chem. 2021, 86, 3555−3564

contributors, which are the HOMO energy of the nucleophile and the LUMO energy of the addition product. This observation suggests that describing general nucleophilicity as a sole function of one nucleophile feature (e.g., HOMO energy) is reductive. This could be done only in specific cases in which $\mathbf{e}_{HOMO}$ and $\mathbf{e}^{+}_{LUMO}$ are colinear, that is, in the case of structurally similar subsets. In these cases, factors contributing to $\mathbf{e}^{+}_{LUMO}$ (change of geometry, overlap integral, mixing of other orbitals, etc.) can be neglected.

Due to the high impact that Mayr's reactivity scale has been having since its development, we foresee that this work will support its implementation in the chemists' everyday effort toward exploring and rationalizing new chemical reactivity.

EXPERIMENTAL SECTION

All computations were performed using the Gaussian 16[38] suite of programs. The nucleophile conformational space was explored manually as most nucleophiles included in this study are small, simple molecules with only few rotatable bonds. Geometry optimizations, vibrational frequencies, and intensities were calculated at the M06-2X/def2TZVP level of theory.[39] All the structures computed in this study are minima as confirmed by vibrational analysis showing no imaginary frequencies. NBO charges were computed using NBO 3.1 implemented in Gaussian 16.[40] Buried volumes were computed using SambVca 2.1.[41] Solvation energies were computed by single-point energy calculation on the M06-2X/def2TZVP geometry at the same theory level with the addition of the SMD[42] solvation model implemented in Gaussian 16. Multidimensional regression analyses were performed using Matlab.[43] Further details are given in the Supporting Information.

ASSOCIATED CONTENT

Supporting Information

The Supporting Information is available free of charge at https://pubs.acs.org/doi/10.1021/acs.joc.0c02952.

Computational methods including parameters of all nucleophiles and solvents, Cartesian coordinates, and data sets (PDF)

AUTHOR INFORMATION

Corresponding Author

Manuel Orlandi − *Department of Chemical Sciences, University of Padova, 35131 Padova, Italy; CIRCC−Consorzio Interuniversitario per le Reattività Chimiche e la Catalisi, 35131 Padova, Italy;* orcid.org/0000-0002-0569-6719; Email: manuel.orlandi@unipd.it

Authors

Margarita Escudero-Casao − *Department of Chemical Sciences, University of Padova, 35131 Padova, Italy; CIRCC−Consorzio Interuniversitario per le Reattività Chimiche e la Catalisi, 35131 Padova, Italy*

Giulia Licini − *Department of Chemical Sciences, University of Padova, 35131 Padova, Italy; CIRCC−Consorzio Interuniversitario per le Reattività Chimiche e la Catalisi, 35131 Padova, Italy;* orcid.org/0000-0001-8304-0443

Complete contact information is available at: https://pubs.acs.org/10.1021/acs.joc.0c02952

Notes

The authors declare no competing financial interest.

ACKNOWLEDGMENTS

We thank Prof. H. Mayr (Ludwig-Maximilians-Universität München) for useful discussions and insights. Computations were performed at the HPC facility of the Computational Chemistry Community of Padova (C3P).

REFERENCES

(1) Ingold, C. K. 266. Significance of tautomerism and of the reactions of aromatic compounds in the electronic theory of organic reactions. *J. Chem. Soc.* **1933**, 1120−1127.

(2) Ingold, C. K. Principles of an Electronic Theory of Organic Reactions. *Chem. Rev.* **1934**, *15*, 225−274.

(3) Swain, C. G.; Scott, C. B. Quantitative Correlation of Relative Rates. Comparison of Hydroxide Ion with Other Nucleophilic Reagents toward Alkyl Halides, Esters, Epoxides and Acyl Halides1. *J. Am. Chem. Soc.* **1953**, *75*, 141−147.

(4) Ritchie, C. D. Nucleophilic reactivities toward cations. *Acc. Chem. Res.* **1972**, *5*, 348−354.

(5) Ritchie, C. D. Cation−anion combination reactions. 26. A review. *Can. J. Chem.* **1986**, *64*, 2239−2250.

(6) For seminal work leading to the formulation of the Mayr−Patz reactivity scale see: (a) Mayr, H.; Schneider, R.; Schade, C.; Bartl, J.; Bederke, R. Addition reactions of diarylcarbenium ions to 2-methyl-1-pentene: kinetic method and reaction mechanism. *J. Am. Chem. Soc.* **1990**, *112*, 4446−4454. (b) Mayr, H.; Schneider, R.; Irrgang, B.; Schade, C. Kinetics of the reactions of the p-methoxy-substituted benzhydryl cation with various alkenes and 1,3-dienes. *J. Am. Chem. Soc.* **1990**, *112*, 4454−4459. (c) Mayr, H.; Schneider, R.; Grabis, U. Linear free energy and reactivity-selectivity relationships in reactions of diarylcarbenium ions with π-nucleophiles. *J. Am. Chem. Soc.* **1990**, *112*, 4460−4467.

(7) (a) Mayr, H.; Patz, M. Scales of Nucleophilicity and Electrophilicity: A System for Ordering Polar Organic and Organometallic Reactions. *Angew. Chem., Int. Ed.* **1994**, *33*, 938−957. (b) Mayr, H.; Kempf, B.; Ofial, A. R. π-Nucleophilicity in Carbon−Carbon Bond-Forming Reactions. *Acc. Chem. Res.* **2003**, *36*, 66−77. (c) Minegishi, S.; Mayr, H. How Constant Are Ritchie's "Constant Selectivity Relationships"? A General Reactivity Scale for n-, π-, and σ-Nucleophiles. *J. Am. Chem. Soc.* **2003**, *125*, 286−295. (d) Mayr, H.; Ofial, A. R. Do general nucleophilicity scales exist? *J. Phys. Org. Chem.* **2008**, *21*, 584−595. (e) Phan, T. B.; Breugst, M.; Mayr, H. Towards a General Scale of Nucleophilicity? *Angew. Chem., Int. Ed.* **2006**, *45*, 3869−3874. . The full Mayr's database is available online at: https://www.cup.lmu.de/oc/mayr/reaktionsdatenbank2

(8) (a) Schindele, C.; Houk, K. N.; Mayr, H. Relationships between Carbocation Stabilities and Electrophilic Reactivity Parameters, E: Quantum Mechanical Studies of Benzhydryl Cation Structures and Stabilities. *J. Am. Chem. Soc.* **2002**, *124*, 11208−11214. (b) Würthwein, E.-U.; Lang, G.; Schappele, L. H.; Mayr, H. Rate-Equilibrium Relationships in Hydride Transfer Reactions: The Role of Intrinsic Barriers. *J. Am. Chem. Soc.* **2002**, *124*, 4084−4092. (c) Mayr, H.; Ofial, A. R. The Reactivity−Selectivity Principle: An Imperishable Myth in Organic Chemistry. *Angew. Chem., Int. Ed.* **2006**, *45*, 1844−1854. (d) Wang, C.; Fu, Y.; Guo, Q.-X.; Liu, L. First-Principles Prediction of Nucleophilicity Parameters for π-Nucleophiles: Implications for Mechanistic Origin of Mayr's Equation. *Chem.—Eur. J.* **2010**, *16*, 2586−2598. (e) Zhuo, L.-G.; Liao, W.; Yu, Z.-X. A Frontier Molecular Orbital Theory Approach to Understanding the Mayr Equation and to Quantifying Nucleophilicity and Electrophilicity by Using HOMO and LUMO Energies. *Asian J. Org. Chem.* **2012**, *1*, 336−345. (f) Chamorro, E.; Duque-Noreña, M.; Notario, R.; Pérez, P. Intrinsic Relative Scales of Electrophilicity and Nucleophilicity. *J. Phys. Chem. A* **2013**, *117*, 2636−2643. (g) Tognetti, V.; Morell, C.; Joubert, L. Quantifying electro/nucleophilicity by partitioning the dual descriptor. *J. Comput. Chem.* **2015**, *36*, 649−659. (h) Liu, S.; Rong, C.; Lu, T. Information Conservation Principle Determines Electrophilicity, Nucleophilicity, and Regioselectivity. *J. Phys. Chem. A* **2014**, *118*, 3698−3704. (i) Pereira, F.; Latino, D. A. R.

S.; Aires-de-Sousa, J. Estimation of Mayr Electrophilicity with a Quantitative Structure−Property Relationship Approach Using Empirical and DFT Descriptors. *J. Org. Chem.* **2011**, *76*, 9312−9319. (j) Kiyooka, S.-i.; Kaneno, D.; Fujiyama, R. Intrinsic reactivity index as a single scale directed toward both electrophilicity and nucleophilicity using frontier molecular orbitals. *Tetrahedron* **2013**, *69*, 4247−4258.

(9) For examples about how the reactivity scale has been employed as a roadmap to find new synthetic transformations see: (a) Gualandi, A.; Mengozzi, L.; Manoni, E.; Giorgio Cozzi, P. From QCA (Quantum Cellular Automata) to Organocatalytic Reactions with Stabilized Carbenium Ions. *Chem. Rec.* **2016**, *16*, 1228−1243. (b) Formica, M.; Rozsar, D.; Su, G.; Farley, A. J. M.; Dixon, D. J. Bifunctional Iminophosphorane Superbase Catalysis: Applications in Organic Synthesis. *Acc. Chem. Res.* **2020**, *53*, 2235−2247. (c) Zhang, J.; Yang, J. D.; Cheng, J. P. A Nucleophilicity Scale for the Reactivity of Diazaphospholenium Hydrides: Structural Insights and Synthetic Applications. *Angew. Chem., Int. Ed.* **2019**, *58*, 5983−5987. (d) Mehdi, M. A.; Bushnell, E. A. C.; Nikoo, S.; Gauld, J. W.; Green, J. R. Generation and Reactions of a Benzodehydrotropylium Ion−Co2-(CO)6 Complex. *ACS Omega* **2019**, *4*, 18600−18608. (e) Um, I.-H.; Kim, M.-Y.; Kang, T.-A.; Dust, J. M. Kinetic Study on SNAr Reaction of 1-(Y-Substituted-phenoxy)-2,4-dinitrobenzenes with Cyclic Secondary Amines in Acetonitrile: Evidence for Cyclic Transition-State Structure. *J. Org. Chem.* **2014**, *79*, 7025−7031. (f) Schreyer, L.; Properzi, R.; List, B. IDPi Catalysis. *Angew. Chem., Int. Ed.* **2019**, *58*, 12761−12777. (g) Voll, C.-C. A.; Swager, T. M. Extended π-Conjugated Structures via Dehydrative C−C Coupling. *J. Am. Chem. Soc.* **2018**, *140*, 17962−17967. (h) Ilic, S.; Alherz, A.; Musgrave, C. B.; Glusac, K. D. Thermodynamic and kinetic hydricities of metal-free hydrides. *Chem. Soc. Rev.* **2018**, *47*, 2809−2836. (i) Bartolo, N. D.; Read, J. A.; Valentín, E. M.; Woerpel, K. A. Reactions of Allylmagnesium Reagents with Carbonyl Compounds and Compounds with C=N Double Bonds: Their Diastereoselectivities Generally Cannot Be Analyzed Using the Felkin−Anh and Chelation-Control Models. *Chem. Rev.* **2020**, *120*, 1513−1619. (j) Murphy, J. J.; Silvi, M.; Melchiorre, P. *Lewis Base Catalysis in Organic Synthesis*; Vedejs, E., Denmark, S. E., Eds.; John Wiley & Sons, 2016; 1, 2 and 3, pp 857−902. (k) Kolishetti, N.; Faust, R. Structure−Reactivity Scales in Carbocationic Polymerizations. *Macromolecules* **2008**, *41*, 9025−9029. (l) Banerjee, S.; Jha, B. N.; De, P.; Emert, J.; Faust, R. Kinetic and Mechanistic Studies of the Polymerization of Isobutylene Catalyzed by $EtAlCl_2$/Bis(2-chloroethyl) Ether Complex in Hexanes. *Macromolecules* **2015**, *48*, 5474−5480. . For examples about its use in the rationalization of the activity of aminocatalysts and their enamine intermediates: (m) Lakhdar, S.; Maji, B.; Mayr, H. Imidazolidinone-Derived Enamines: Nucleophiles with Low Reactivity. *Angew. Chem., Int. Ed.* **2012**, *51*, 5739−5742. (n) Mayr, H.; Lakhdar, S.; Maji, B.; Ofial, A. R. A quantitative approach to nucleophilic organocatalysis. *Beilstein J. Org. Chem.* **2012**, *8*, 1458−1478. (o) An, F.; Maji, B.; Min, E.; Ofial, A. R.; Mayr, H. Basicities and Nucleophilicities of Pyrrolidines and Imidazolidinones Used as Organocatalysts. *J. Am. Chem. Soc.* **2020**, *142*, 1526−1547.

(10) (a) Contreras, R.; Andres, J.; Safont, V. S.; Campodonico, P.; Santos, J. G. A Theoretical Study on the Relationship between Nucleophilicity and Ionization Potentials in Solution Phase. *J. Phys. Chem. A* **2003**, *107*, 5588−5593. (b) Domingo, L. R.; Pérez, P.; Contreras, R. Reactivity of the carbon−carbon double bond towards nucleophilic additions. A DFT analysis. *Tetrahedron* **2004**, *60*, 6585−6591. (c) Gázquez, J. L.; Cedillo, A.; Vela, A. Electrodonating and Electroaccepting Powers. *J. Phys. Chem. A* **2007**, *111*, 1966−1970. (d) Kiyooka, S.-i.; Kaneno, D.; Fujiyama, R. Parr's index to describe both electrophilicity and nucleophilicity. *Tetrahedron Lett.* **2013**, *54*, 339−342. (e) Kiyooka, S.-i.; Kaneno, D.; Fujiyama, R. Intrinsic reactivity index as a single scale directed toward both electrophilicity and nucleophilicity using frontier molecular orbitals. *Tetrahedron* **2013**, *69*, 4247−4258. (f) Jaramillo, P.; Pérez, P.; Fuentealba, P. Relationship between basicity and nucleophilicity. *J. Phys. Org. Chem.* **2007**, *20*, 1050−1057. (g) Domingo, L. R.; Chamorro, E.; Pérez, P. Understanding the Reactivity of Captodative Ethylenes in Polar Cycloaddition Reactions. A Theoretical Study. *J. Org. Chem.* **2008**, *73*, 4615−4624. (h) Domingo, L. R.; Pérez, P. The nucleophilicity N index in organic chemistry. *Org. Biomol. Chem.* **2011**, *9*, 7168−7175.

(11) (a) Allgäuer, D. S.; Jangra, H.; Asahara, H.; Li, Z.; Chen, Q.; Zipse, H.; Ofial, A. R.; Mayr, H. Quantification and Theoretical Analysis of the Electrophilicities of Michael Acceptors. *J. Am. Chem. Soc.* **2017**, *139*, 13318−13329. (b) Mood, A.; Tavakoli, M.; Gutman, E.; Kadish, D.; Baldi, P.; Van Vranken, D. L. Methyl Anion Affinities of the Canonical Organic Functional Groups. *J. Org. Chem.* **2020**, *85*, 4096−4102. (c) Mayer, R. J.; Ofial, A. R. Nucleophilicity of Glutathione: A Link to Michael Acceptor Reactivities. *Angew. Chem., Int. Ed.* **2019**, *58*, 17704−17708.

(12) (a) Santiago, C. B.; Guo, J.-Y.; Sigman, M. S. Predictive and mechanistic multivariate linear regression models for reaction development. *Chem. Sci.* **2018**, *9*, 2398−2412. (b) Sigman, M. S.; Harper, K. C.; Bess, E. N.; Milo, A. The Development of Multidimensional Analysis Tools for Asymmetric Catalysis and Beyond. *Acc. Chem. Res.* **2016**, *49*, 1292−1301. (c) Reid, J. P.; Sigman, M. S. Holistic prediction of enantioselectivity in asymmetric catalysis. *Nature* **2019**, *571*, 343−348. (d) Orlandi, M.; Coelho, J. A. S.; Hilton, M. J.; Toste, F. D.; Sigman, M. S. Parametrization of Noncovalent Interactions for Transition State Interrogation Applied to Asymmetric Catalysis. *J. Am. Chem. Soc.* **2017**, *139*, 6803−6806. (e) Sandford, C.; Fries, L. R.; Ball, T. E.; Minteer, S. D.; Sigman, M. S. Mechanistic Studies into the Oxidative Addition of Co(I) Complexes: Combining Electroanalytical Techniques with Parameterization. *J. Am. Chem. Soc.* **2019**, *141*, 18877−18889. (f) Ravasco, J. M. J. M.; Coelho, J. A. S. Predictive Multivariate Models for Bioorthogonal Inverse-Electron Demand Diels−Alder Reactions. *J. Am. Chem. Soc.* **2020**, *142*, 4235−4241.

(13) Falivene, L.; Cao, Z.; Petta, A.; Serra, L.; Poater, A.; Oliva, R.; Scarano, V.; Cavallo, L. Towards the online computer-aided design of catalytic pockets. *Nat. Chem.* **2019**, *11*, 872−879.

(14) Verloop, A. *Drug Design*; Ariens, E. J., Ed.; Academic Press: New York, 1976, Vol. *III*

(15) Reed, A. E.; Curtiss, L. A.; Weinhold, F. Intermolecular interactions from a natural bond orbital, donor-acceptor viewpoint. *Chem. Rev.* **1988**, *88*, 899−926.

(16) Singh, U. C.; Kollman, P. A. An approach to computing electrostatic charges for molecules. *J. Comput. Chem.* **1984**, *5*, 129−145.

(17) Albright, T. A.; Burdett, J. K.; Whangbo, M.-H. *Orbital Interactions in Chemistry*, 2nd ed.; Wiley: Hoboken, NJ, 2013.

(18) Geerlings, P.; De Proft, F.; Langenaeker, W. Conceptual Density Functional Theory. *Chem. Rev.* **2003**, *103*, 1793−1874.

(19) Marenich, A. V.; Cramer, C. J.; Truhlar, D. G. Universal Solvation Model Based on Solute Electron Density and on a Continuum Model of the Solvent Defined by the Bulk Dielectric Constant and Atomic Surface Tensions. *J. Phys. Chem. B* **2009**, *113*, 6378−6396.

(20) (a) Mayr, H.; Bug, T.; Gotta, M. F.; Hering, N.; Irrgang, B.; Janker, B.; Kempf, B.; Loos, R.; Ofial, A. R.; Remennikov, G.; Schimmel, H. Reference Scales for the Characterization of Cationic Electrophiles and Neutral Nucleophiles. *J. Am. Chem. Soc.* **2001**, *123*, 9500−9512. (b) Ammer, J.; Nolte, C.; Mayr, H. Free Energy Relationships for Reactions of Substituted Benzhydrylium Ions: From Enthalpy over Entropy to Diffusion Control. *J. Am. Chem. Soc.* **2012**, *134*, 13902−13911.

(21) (a) Lakhdar, S.; Westermaier, M.; Terrier, F.; Goumont, R.; Boubaker, T.; Ofial, A. R.; Mayr, H. Nucleophilic Reactivities of Indoles. *J. Org. Chem.* **2006**, *71*, 9088−9095. (b) Nigst, T. A.; Westermaier, M.; Ofial, A. R.; Mayr, H. Nucleophilic Reactivities of Pyrroles. *Eur. J. Org. Chem.* **2008**, 2369−2374.

(22) Leonov, A.; Timofeeva, D.; Ofial, A.; Mayr, H. Metal Enolates − Enamines − Enol Ethers: How Do Enolate Equivalents Differ in Nucleophilic Reactivity? *Synthesis* **2019**, *51*, 1157−1170.

(23) (a) Kempf, B.; Hampel, N.; Ofial, A. R.; Mayr, H. Structure−Nucleophilicity Relationships for Enamines. *Chem.—Eur. J.* **2003**, *9*,

https://dx.doi.org/10.1021/acs.joc.0c02952
J. Org. Chem. 2021, 86, 3555−3564

2209−2218. (b) Maji, B.; Lakhdar, S.; Mayr, H. Nucleophilicity Parameters of Enamides and Their Implications for Organocatalytic Transformations. *Chem.—Eur. J.* **2012**, *18*, 5732−5740. (c) Timofeeva, D. S.; Mayer, R. J.; Mayer, P.; Ofial, A. R.; Mayr, H. Which Factors Control the Nucleophilic Reactivities of Enamines? *Chem.—Eur. J.* **2018**, *24*, 5901−5910.

(24) (a) Appel, R.; Hartmann, N.; Mayr, H. Scope and Limitations of Cyclopropanations with Sulfur Ylides. *J. Am. Chem. Soc.* **2010**, *132*, 17894−17900. (b) Appel, R.; Mayr, H. Nucleophilic Reactivities of Sulfur Ylides and Related Carbanions: Comparison with Structurally Related Organophosphorus Compounds. *Chem.—Eur. J.* **2010**, *16*, 8610−8614.

(25) (a) Maji, B.; Breugst, M.; Mayr, H. N-Heterocyclic Carbenes: Organocatalysts with Moderate Nucleophilicity but Extraordinarily High Lewis Basicity. *Angew. Chem., Int. Ed.* **2011**, *50*, 6915−6919. (b) Levens, A.; An, F.; Breugst, M.; Mayr, H.; Lupton, D. W. Influence of the N-Substituents on the Nucleophilicity and Lewis Basicity of N-Heterocyclic Carbenes. *Org. Lett.* **2016**, *18*, 3566−3569.

(26) (a) Lucius, R.; Loos, R.; Mayr, H. Kinetic Studies of Carbocation−Carbanion Combinations: Key to a General Concept of Polar Organic Reactivity. *Angew. Chem., Int. Ed.* **2002**, *41*, 91−95. (b) Bug, T.; Mayr, H. Nucleophilic Reactivities of Carbanions in Water: The Unique Behavior of the Malodinitrile Anion. *J. Am. Chem. Soc.* **2003**, *125*, 12980−12986. (c) Bug, T.; Lemek, T.; Mayr, H. Nucleophilicities of Nitroalkyl Anions. *J. Org. Chem.* **2004**, *69*, 7565−7576. (d) Kaumanns, O.; Appel, R.; Lemek, T.; Seeliger, F.; Mayr, H. Nucleophilicities of the Anions of Arylacetonitriles and Arylpropionitriles in Dimethyl Sulfoxide. *J. Org. Chem.* **2009**, *74*, 75−81. (e) Corral-Bautista, F.; Mayr, H. Quantification of the Nucleophilic Reactivities of Ethyl Arylacetate Anions. *Eur. J. Org. Chem.* **2013**, 4255−4261. (f) Zhang, Z.; Puente, Á.; Wang, F.; Rahm, M.; Mei, Y.; Mayr, H.; Prakash, G. K. S. The Nucleophilicity of Persistent α-Monofluoromethide Anions. *Angew. Chem., Int. Ed.* **2016**, *55*, 12845−12849. (g) Corral-Bautista, F.; Mayr, H. Quantification of the Nucleophilic Reactivities of Cyclic β-Keto Ester Anions. *Eur. J. Org. Chem.* **2015**, 7594−7601.

(27) (a) Brotzel, F.; Chu, Y. C.; Mayr, H. Nucleophilicities of Primary and Secondary Amines in Water. *J. Org. Chem.* **2007**, *72*, 3679−3688. (b) Phan, T. B.; Nolte, C.; Kobayashi, S.; Ofial, A. R.; Mayr, H. Can One Predict Changes from SN1 to SN2 Mechanisms? *J. Am. Chem. Soc.* **2009**, *131*, 11392−11401. (c) Kanzian, T.; Nigst, T. A.; Maier, A.; Pichl, S.; Mayr, H. Nucleophilic Reactivities of Primary and Secondary Amines in Acetonitrile. *Eur. J. Org. Chem.* **2009**, 6379−6385. (d) Brotzel, F.; Kempf, B.; Singer, T.; Zipse, H.; Mayr, H. Nucleophilicities and Carbon Basicities of Pyridines. *Chem.—Eur. J.* **2007**, *13*, 336−345. (e) Breugst, M.; Corral Bautista, F.; Mayr, H. Nucleophilic Reactivities of the Anions of Nucleobases and Their Subunits. *Chem.—Eur. J.* **2012**, *18*, 127−137.

(28) (a) Breugst, M.; Tokuyasu, T.; Mayr, H. Nucleophilic Reactivities of Imide and Amide Anions. *J. Org. Chem.* **2010**, *75*, 5250−5258. (b) Breugst, M.; Mayr, H. Ambident Reactivities of Pyridone Anions. *J. Am. Chem. Soc.* **2010**, *132*, 15380−15389.

(29) (a) Schaller, H. F.; Tishkov, A. A.; Feng, X.; Mayr, H. Direct Observation of the Ionization Step in Solvolysis Reactions: Electrophilicity versus Electrofugality of Carbocations. *J. Am. Chem. Soc.* **2008**, *130*, 3012−3022. (b) Mayer, R. J.; Breugst, M.; Hampel, N.; Ofial, A. R.; Mayr, H. Ambident Reactivity of Phenolate Anions Revisited: A Quantitative Approach to Phenolate Reactivities. *J. Org. Chem.* **2019**, *84*, 8837−8858. (c) Duan, X.-H.; Maji, B.; Mayr, H. Characterization of the nucleophilic reactivities of thiocarboxylate, dithiocarbonate and dithiocarbamate anions. *Org. Biomol. Chem.* **2011**, *9*, 8046−8050. (d) Baidya, M.; Kobayashi, S.; Mayr, H. Nucleophilicity and Nucleofugality of Phenylsulfinate ($PhSO_2^-$): A Key to Understanding its Ambident Reactivity. *J. Am. Chem. Soc.* **2010**, *132*, 4796−4805.

(30) $\mathbf{E}_{PA}$ correlates with the corresponding Gibbs free energies $\mathbf{G}_{PA}$ (R^2 = 0.99), suggesting that thermal corrections are negligible in this context.

(31) (a) Mayr, H.; Ammer, J.; Baidya, M.; Maji, B.; Nigst, T. A.; Ofial, A. R.; Singer, T. Scales of Lewis Basicities toward C-Centered Lewis Acids (Carbocations). *J. Am. Chem. Soc.* **2015**, *137*, 2580−2599. (b) Arnett, E. M. Gas-phase proton transfer. Breakthrough for solution chemistry. *Acc. Chem. Res.* **1973**, *6*, 404−409.

(32) (a) Bordwell, F. G.; Hughes, D. L. Direct relationship between nucleophilicity and basicity in SN_2 reactions of fluorenyl anions with benzyl chloride in dimethyl sulfoxide solution. *J. Org. Chem.* **1980**, *45*, 3314−3320. (b) Bordwell, F. G.; Hughes, D. L. Rate-equilibrium relationships for reactions of families of carbanion nucleophiles with N-benzyl-N,N-dimethylanilinium cations and with alkyl chlorides, bromides, and iodides. *J. Am. Chem. Soc.* **1986**, *108*, 7300−7309. (c) Bordwell, F. G.; Cripe, T. A.; Hughes, D. L. Nucleophilicity, Basicity, and the Brønsted Equation. *Nucleophilicity*; American Chemical Society, 1987.

(33) (a) Berger, S. T. A.; Ofial, A. R.; Mayr, H. Inverse Solvent Effects in Carbocation Carbanion Combination Reactions: The Unique Behavior of Trifluoromethylsulfonyl Stabilized Carbanions. *J. Am. Chem. Soc.* **2007**, *129*, 9753−9761. (b) Appel, R.; Loos, R.; Mayr, H. Nucleophilicity Parameters for Phosphoryl-Stabilized Carbanions and Phosphorus Ylides: Implications for Wittig and Related Olefination Reactions. *J. Am. Chem. Soc.* **2009**, *131*, 704−714. (c) Lucius, R.; Mayr, H. Constant Selectivity Relationships of Addition Reactions of Carbanions. *Angew. Chem., Int. Ed.* **2000**, *39*, 1995−1997.

(34) (a) Horn, M.; Mayr, H. A comprehensive view on stabilities and reactivities of triarylmethyl cations (tritylium ions). *J. Phys. Org. Chem.* **2012**, *25*, 979−988. (b) Ofial, A. R. Benzhydrylium and tritylium ions: complementary probes for examining ambident nucleophiles. *Pure Appl. Chem.* **2015**, *87*, 341−351.

(35) Lakhdar, S.; Ofial, A. R.; Mayr, H. Reactivity parameters for rationalizing iminium-catalyzed reactions. *J. Phys. Org. Chem.* **2010**, *23*, 886−892.

(36) Mayr, H.; Breugst, M.; Ofial, A. R. Farewell to the HSAB Treatment of Ambident Reactivity. *Angew. Chem., Int. Ed.* **2011**, *50*, 6470−6505.

(37) (a) Zahrt, A. F.; Athavale, S. V.; Denmark, S. E. Quantitative Structure−Selectivity Relationships in Enantioselective Catalysis: Past, Present, and Future. *Chem. Rev.* **2019**, *120*, 1620−1689. (b) Reid, J. P.; Sigman, M. S. Holistic prediction of enantioselectivity in asymmetric catalysis. *Nature* **2019**, *571*, 343−348. (c) Werth, J.; Sigman, M. S. Connecting and Analyzing Enantioselective Bifunctional Hydrogen Bond Donor Catalysis Using Data Science Tools. *J. Am. Chem. Soc.* **2020**, *142*, 16382−16391. (d) Zahrt, A. F.; Henle, J. J.; Rose, B. T.; Wang, Y.; Darrow, W. T.; Denmark, S. E. Prediction of higher-selectivity catalysts by computer-driven workflow and machine learning. *Science* **2019**, *363*, No. eaau5631.

(38) Frisch, M. J.; Trucks, G. W.; Schlegel, H. B.; Scuseria, G. E.; Robb, M. A.; Cheeseman, J. R.; Scalmani, G.; Barone, V.; Petersson, G. A.; Nakatsuji, H.; Li, X.; Caricato, M.; Marenich, A. V.; Bloino, J.; Janesko, B. G.; Gomperts, R.; Mennucci, B.; Hratchian, H. P.; Ortiz, J. V.; Izmaylov, A. F.; Sonnenberg, J. L.; Williams-Young, D.; Ding, F.; Lipparini, F.; Egidi, F.; Goings, J.; Peng, B.; Petrone, A.; Henderson, T.; Ranasinghe, D.; Zakrzewski, V. G.; Gao, J.; Rega, N.; Zheng, G.; Liang, W.; Hada, M.; Ehara, M.; Toyota, K.; Fukuda, R.; Hasegawa, J.; Ishida, M.; Nakajima, T.; Honda, Y.; Kitao, O.; Nakai, H.; Vreven, T.; Throssell, K.; Montgomery, J. A., Jr.; Peralta, J. E.; Ogliaro, F.; Bearpark, M. J.; Heyd, J. J.; Brothers, E. N.; Kudin, K. N.; Staroverov, V. N.; Keith, T. A.; Kobayashi, R.; Normand, J.; Raghavachari, K.; Rendell, A. P.; Burant, J. C.; Iyengar, S. S.; Tomasi, J.; Cossi, M.; Millam, J. M.; Klene, M.; Adamo, C.; Cammi, R.; Ochterski, J. W.; Martin, R. L.; Morokuma, K.; Farkas, O.; Foresman, J. B.; Fox, D. J. *Gaussian 16*, Revision C.01; Gaussian, Inc.: Wallingford CT, 2016.

(39) Zhao, Y.; Truhlar, D. G. The M06 suite of density functionals for main group thermochemistry, thermochemical kinetics, noncovalent interactions, excited states, and transition elements: two new functionals and systematic testing of four M06-class functionals and 12 other functionals. *Theor. Chem. Acc.* **2008**, *120*, 215−241.

https://dx.doi.org/10.1021/acs.joc.0c02952
J. Org. Chem. 2021, 86, 3555−3564

(40) Glendening, E. D.; Reed, A. E.; Carpenter, J. E.; Weinhold, F. *NBO* Version 3.1.
(41) Falivene, L.; Cao, Z.; Petta, A.; Serra, L.; Poater, A.; Oliva, R.; Scarano, V.; Cavallo, L. Towards the online computer-aided design of catalytic pockets. *Nat. Chem.* **2019**, *11*, 872−879.
(42) Marenich, A. V.; Cramer, C. J.; Truhlar, D. G. Universal solvation model based on solute electron density and a continuum model of the solvent defined by the bulk dielectric constant and atomic surface tensions. *J. Phys. Chem. B* **2009**, *113*, 6378−6396.
(43) *MATLAB and Statistics Toolbox Release R2020a*; The MathWorks, Inc., Natick, Massachusetts, United States.

https://dx.doi.org/10.1021/acs.joc.0c02952
J. Org. Chem. 2021, 86, 3555−3564